# Assessment of Sea Ice Extent in CMIP6 With Comparison to Observations and CMIP5

Qi Shu[1,2,3] [iD], Qiang Wang[4] [iD], Zhenya Song[1,2,3] [iD], Fangli Qiao[1,2,3] [iD], Jiechen Zhao[5] [iD], Min Chu[6] [iD], and Xinfang Li[1]

[1]First Institute of Oceanography, Ministry of Natural Resources, Qingdao, China, [2]Laboratory for Regional Oceanography and Numerical Modeling, Qingdao National Laboratory for Marine Science and Technology, Qingdao, China, [3]Key Laboratory of Marine Science and Numerical Modeling, Ministry of Natural Resources, Qingdao, China, [4]Alfred Wegener Institute Helmholtz Centre for Polar and Marine Research (AWI), Bremerhaven, Germany, [5]National Marine Environmental Forecasting Center, Beijing, China, [6]Beijing Climate Center, China Meteorological Administration, Beijing, China

**Abstract** Both the Arctic and Antarctic sea ice extents (SIEs) from 44 coupled models in the Coupled Model Intercomparison Project Phase 6 (CMIP6) are evaluated by comparing them with observations and CMIP5 results. The CMIP6 multimodel mean can adequately reproduce the seasonal cycles of both the Arctic and Antarctic SIE. The observed Arctic September SIE declining trend ($-0.82 \pm 0.18$ million $km^2$ per decade) between 1979 and 2014 is slightly underestimated in CMIP6 models ($-0.70 \pm 0.06$ million $km^2$ per decade). The observed weak but significant upward trend of the Antarctic SIE is not captured, which was an issue already in the CMIP5 phase. Compared with CMIP5 models, CMIP6 models have lower intermodel spreads in SIE mean values and trends, although their SIE biases are relatively larger. The CMIP6 models did not reproduce the new summer tendencies after 2000, including the faster decline of Arctic SIE and the larger interannual variability in Antarctic SIE.

## 1. Introduction

Sea ice plays an important role in the Earth's climate system. It modulates the Earth's energy balance, inhibits ocean-atmosphere heat, momentum, and gas exchanges and affects atmosphere and ocean circulations. Arctic sea ice has been dramatically influenced by the ongoing climate change. Satellite observations show that pan-Arctic sea ice extent (SIE) has declined across all seasons (Stroeve & Notz, 2018). Arctic sea ice age, thickness, and drift have all experienced considerable changes (Kwok & Cunningham, 2015; Maslanik et al., 2011; Olason & Notz, 2014).

The situation is quite different for Antarctic (Southern Ocean) SIE (Comiso, Gersten, et al., 2017; Parkinson & Cavalieri, 2012). Satellite data show that total Antarctic SIE had a slightly positive trend over the past four decades (1979–2018) (Parkinson, 2019), with rapid ice loss in the Amundsen and Bellingshausen seas (Holland, 2014). The reason for the observed increase in Antarctic total SIE is still under debate.

Coupled climate models are the primary tools that are used to study sea ice evolution and potential environmental impacts of sea ice decline. The Coupled Model Intercomparison Project (CMIP) provides a very useful framework for the modeling community to assess performance of sea ice simulations in state-of-the-art climate models in order to improve model fidelity. Stroeve et al. (2012) compared Arctic SIE from climate models participating in CMIP Phase 5 (CMIP5) and that from CMIP Phase 3 (CMIP3) models with observations. They concluded that the multimodel mean (MMM) trend and seasonal cycle of Arctic SIE in CMIP5 models are more consistent with observations than in CMIP3 models, while the trends from most ensemble members and models remain smaller than the observed value. Turner et al. (2013) and Shu et al. (2015) assessed Antarctic sea ice simulations in CMIP5 and found that the models can adequately reproduce the seasonal cycle of Antarctic SIE. However, intermodel spread is large and most CMIP5 models are unable to reproduce the observed positive Antarctic SIE trend.

Sea ice simulations from the state-of-the-art climate models participating in the CMIP Phase 6 (CMIP6) have been released. In this study we evaluate CMIP6 sea ice simulations by comparing them with CMIP5 simulations and satellite observations.

## 2. Data and Methods

Monthly sea ice output of CMIP6 and CMIP5 historical runs were used in this study. Historical sea ice simulations from 46 CMIP6 coupled models have been released through the CMIP6 Commodity Governance web interfaces. SIE from five models, and sea ice concentration (SIC) from the other 41 models have been provided. For latter 41 models, we derived the SIE from the SIC data using their original model grids without any remapping. SIE was computed as the total area of all the grid cells that have SIC exceeding 15%. As two models (MIROC6 and MIROC-ES2L) have dramatically large SIE biases in the Antarctic, we excluded them during our analysis. These models have unrealistically low Antarctic SIE due to their too warm sea surface temperature caused by the underestimation of midlevel cloud cover and the excess downward shortwave radiation (Tatebe et al., 2019). We assessed 307 available realizations from the other 44 CMIP6 models. Detailed information about these CMIP6 models can be found in Table S1 in the supporting information.

To investigate the changes of model skills in representing SIE stepping from CMIP5 to CMIP6, we compared CMIP6 results with the first realizations from 49 CMIP5 models. Information about these 49 CMIP5 models can be found in Shu et al. (2015). We analyzed model results from 1979 (start of the continuous sea ice satellite record) to the end of the historical runs (2005 for CMIP5 and 2014 for CMIP6 simulations).

Two satellite-derived SIE data sets were used. The first is from University of Bremen (UBremen) (https://seaice.uni-bremen.de/sea-ice-concentration-amsr-eamsr2/time-series/) (Spreen et al., 2008). It is composed of observations from different sensors, using different sea ice concentration retrieval algorithms and adaptations to each other using certain overlap periods. The second is from the National Snow and Ice Data Centre (NSIDC) (http://nsidc.org/data/g02135.html) (Fetterer et al., 2017). The satellite-observed SIC data set from NSIDC (http://nsidc.org/data/seaice/) was also used in this study (Cavalieri et al., 1996), which is retrieved using the National Aeronautics and Space Administration team algorithm. To investigate Arctic surface warming trends, we also used monthly surface air temperature from CMIP6 models and ERA5 reanalysis (https://cds.climate.copernicus.eu/#!/home) (Copernicus Climate Change Service (C3S), 2017).

Models in CMIP6 differ in their number of realizations. To avoid biasing the MMM toward the models with a higher number of realizations, we calculated MMM using the multirealization mean of each CMIP6 model, instead of taking the mean of all realizations.

## 3. Results

### 3.1. Climatology and Seasonal Cycle

The seasonal cycles of Arctic SIE from CMIP5 and CMIP6 simulations and the observations are depicted in Figure 1a. It shows that all of them reach maximum in March and minimum in September, indicating the ability of CMIP6 and CMIP5 models to adequately reproduce the seasonal cycle of Arctic SIE. The SIE biases are similar in the CMIP6 and CMIP5, which are relatively larger in winter than in summer (Figure 1a). March SIEs from UBremen, NSIDC, CMIP5, and CMIP6 for 1979 to 2005 are 15.49, 15.59, 17.25, and 17.29 million km$^2$, respectively (Table 1). Seven CMIP6 models (CAMS-CSM1-0, E3SM-1-0, E3SM-1-1, E3SM-1-1-ECA, GISS-E2-1-G, GISS-E2-1-G-CC, and GISS-E2-1-H) have too high (more than 20 million km$^2$) Arctic SIE in March (Figure S1a), which causes the overestimation of CMIP6 MMM SIE. The large biases in the CAMS-CSM1-0 and E3SM models are possibly due to the models' underestimation of the northward ocean heat transport associated with low strength of Atlantic Meridional Overturning Circulation (Golaz et al., 2019; Wei et al., 2018). September SIEs from UBremen, NSIDC, CMIP5, and CMIP6 for 1979 to 2005 are 6.76, 6.75, 6.85, and 7.54 million km$^2$, respectively (Table 1). The comparison indicates that CMIP6 simulations have relatively larger biases in summer. Most CMIP6 models have larger SIE than observed in September (Figure S1b). However, both CMIP6 and CMIP5 MMM SIEs are within the 15% uncertainty range of satellite-derived SIE for all months averaged over 1979–2005. Intermodel spread is large in CMIP5 models (Stroeve et al., 2012; Shu et al., 2015), especially in winter. While it remains large in CMIP6 models, it is reduced in summer (as shown by the shading in Figure 1a). One standard deviation (STD, an indication of model spread) of summer (July–September) SIE is 1.58 and 1.26 million km$^2$ in CMIP5 and CMIP6, respectively (Table 1).
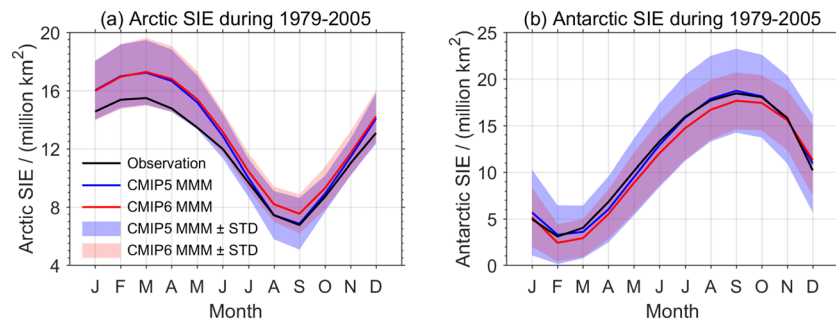
**Figure 1.** Climatology of CMIP5 and CMIP6 multimodel mean (MMM) sea ice extent (SIE) during 1979–2005 for the (a) Arctic and (b) Antarctic. Shading shows the range of one standard deviation (STD); blue for CMIP5 and pink for CMIP6. Climatological SIE from UBremen satellite dataset is shown with black lines.

Figure 1b shows the seasonal cycles of Antarctic SIE from CMIP5 and CMIP6 simulations and the observations. It indicates that CMIP6 models can well reproduce the observed SIE seasonal cycle in the Antarctic, which is similar to CMIP5 models, although the (negative) biases are slightly larger in CMIP6 models. Previous studies by Turner et al. (2013) and Shu et al. (2015) concluded that Antarctic SIE intermodel spread is large in CMIP5 models. One improvement from CMIP5 to CMIP6 is that the intermodel spread is reduced for all the seasons (as shown by the light shading in Figure 1b). The intermodel spread of annual mean Antarctic SIE is 4.24 and 3.02 million $km^2$ in the CMIP5 and CMIP6, respectively, equivalent to a reduction of about 29% from CMIP5 to CMIP6. However, the CMIP6 intermodel spread is still quite large, especially in summer (Figure S2a).

### 3.2. Linear Trend

The linear trends of Arctic SIE during 1979–2005 in CMIP6 and CMIP5 are very similar and both fit the satellite observations well (Figures 2a, 2b, 3a, and 3b, Table 1, and Figure S1c). March Arctic SIE trends from

**Table 1**
*Different Sea Ice Indexes From Satellite Observations, CMIP5, and CMIP6*

| Index | UBremen | NSIDC | CMIP5 | CMIP6 |
|---|---|---|---|---|
| Arctic SIE in March during 1979 to 2005 (million $km^2$) | 15.49 | 15.59 | 17.25 | 17.29 |
| Arctic SIE in September during 1979 to 2005 (million $km^2$) | 6.76 | 6.75 | 6.85 | 7.54 |
| Arctic SIE in March during 1979 to 2014 (million $km^2$) | 15.31 | 15.41 | — | 17.08 |
| Arctic SIE in September during 1979 to 2014 (million $km^2$) | 6.30 | 6.27 | — | 7.18 |
| The STD of Arctic mean SIE in summer (JAS) average from 1979 to 2005 (million $km^2$) | — | — | 1.58 | 1.26 |
| Arctic March SIE trend during 1979 to 2005 (million $km^2$ per decade) | −0.32 (0.12) | −0.38 (0.11) | −0.31 (0.05) | −0.42 (0.06) |
| Arctic September SIE trend during 1979 to 2005 (million $km^2$ per decade) | −0.54 (0.22) | −0.54 (0.22) | −0.58 (0.09) | −0.61 (0.10) |
| Arctic September SIE trend during 2000 to 2014 (million $km^2$ per decade) | −1.36 (0.79) | −1.39 (0.76) | — | −0.77 (0.07) |
| Arctic March SIE trend during 1979 to 2014 (million $km^2$ per decade) | −0.35 (0.09) | −0.38 (0.08) | — | −0.45 (0.03) |
| Arctic September SIE trend during 1979 to 2014 (million $km^2$ per decade) | −0.82 (0.18) | −0.83 (0.18) | — | −0.70 (0.06) |
| The STD of Arctic March SIE trend during 1979 to 2005 (million $km^2$ per decade) | — | — | 0.25 | 0.24 |
| The STD of Arctic September SIE trend during 1979 to 2005 (million $km^2$ per decade) | — | — | 0.34 | 0.26 |
| Antarctic SIE in March during 1979 to 2014 (million $km^2$) | 4.09 | 4.06 | — | 2.79 |
| Antarctic SIE in September during 1979 to 2014 (million $km^2$) | 18.60 | 18.58 | — | 17.47 |
| The STD of Antarctic mean SIE average from 1979 to 2005 (million $km^2$) | — | — | 4.24 | 3.02 |
| Antarctic annual SIE trend during 1979 to 2005 (million $km^2$ per decade) | 0.13 (0.10) | 0.14 (0.10) | −0.34 (0.03) | −0.35 (0.03) |
| Antarctic March SIE trend during 1979 to 2005 (million $km^2$ per decade) | 0.26 (0.18) | 0.23 (0.17) | −0.21 (0.04) | −0.23 (0.03) |
| Antarctic September SIE trend during 1979 to 2005 (million $km^2$ per decade) | 0.10 (0.16) | 0.10 (0.16) | −0.45 (0.04) | −0.43 (0.03) |
| Antarctic March SIE trend during 1979 to 2014 (million $km^2$ per decade) | 0.23 (0.15) | 0.21 (0.15) | — | −0.23 (0.02) |
| Antarctic September SIE trend during 1979 to 2014 (million $km^2$ per decade) | 0.24 (0.12) | 0.23 (0.12) | — | −0.43 (0.02) |
| The STD of Antarctic March detrended SIE during 2000 to 2014 (million $km^2$) | 0.60 | 0.59 | — | 0.47 |
| The STD of Antarctic March SIE trend during 1979 to 2005 (million $km^2$ per decade) | — | — | 0.29 | 0.19 |
| The STD of Antarctic September SIE trend during 1979 to 2005 (million $km^2$ per decade) | — | — | 0.58 | 0.33 |

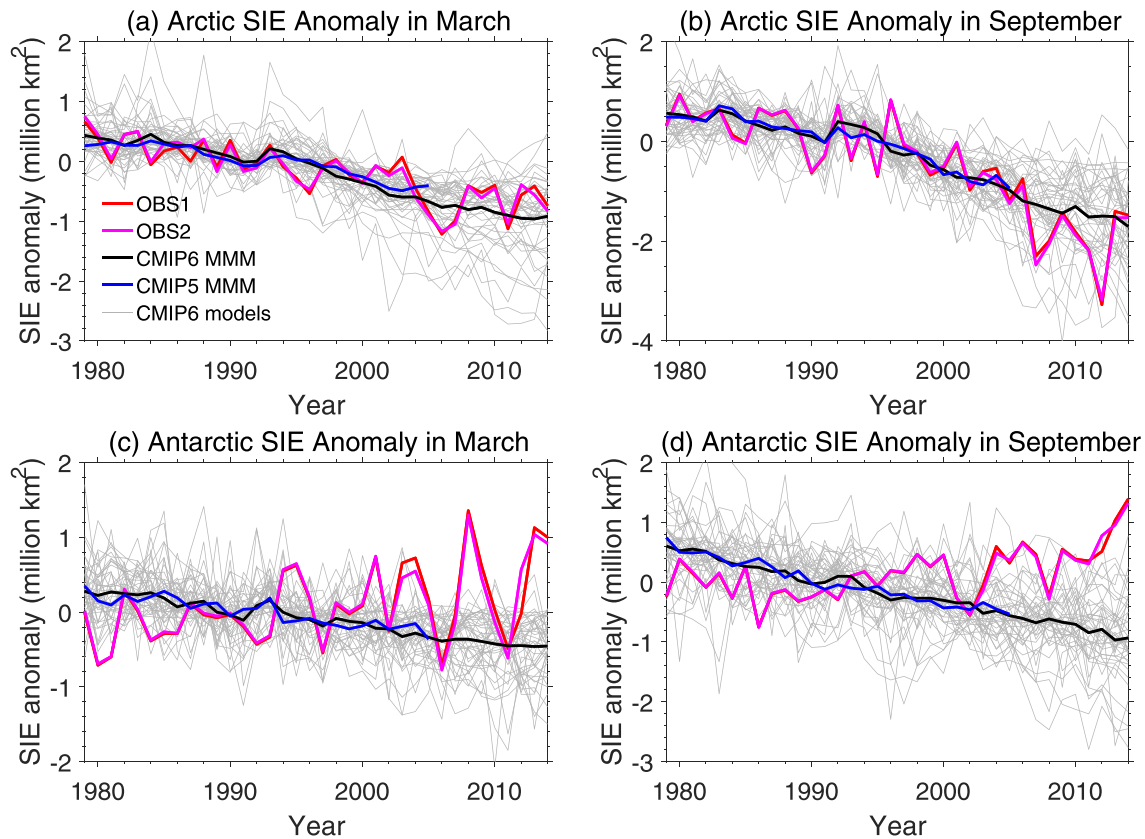*Note.* The values in parentheses indicate the significant levels.

**Figure 2.** Satellite-derived and CMIP5/CMIP6-simulated sea ice extent (SIE) anomalies for (left) March and (right) September for the (upper) Arctic and (bottom) Antarctic. Anomalies are calculated with respect to the mean from 1979–2005. OBS1 and OBS2 indicate satellite observations from UBremen and NSIDC, respectively. MMM indicates multimodel mean.

UBremen, NSIDC, CMIP5, and CMIP6 for 1979 to 2005 are $-0.32$ ($\pm0.12$), $-0.38$ ($\pm0.11$), $-0.31$ ($\pm0.05$), and $-0.42$ ($\pm0.06$) million km$^2$ per decade, respectively. The September SIE trend in this period is $-0.54$ ($\pm0.22$) million km$^2$ per decade from both UBremen and NSIDC, and $-0.58$ ($\pm0.09$) and $-0.61$ ($\pm0.10$) million km$^2$ per decade from CMIP5 and CMIP6, respectively.

Satellite observations show that there is an acceleration of changes in the Arctic SIE in September (Comiso, Meier, et al., 2017). Figure 2b shows that the observed Arctic SIE in September declined faster after 2000 compared with the period before 2000. This faster declining trend is absent in CMIP6 simulations (Figures 2b and 3e, Table 1, and Figure S1d). For 2000 to 2014, September SIE trends from UBremen and NSIDC are $-1.36$ ($\pm0.79$) and $-1.39$ ($\pm0.76$) million km$^2$ per decade, respectively (Table 1). However, the trend is only $-0.77$ ($\pm0.07$) million km$^2$ per decade in the CMIP6 simulations (Table 1). Figure 3e indicates that most (83%) of CMIP6 realizations underestimate the Arctic SIE declining trend in this period. Only six CMIP6 models (CanESM5-CanOE, E3SM-1-0, E3SM-1-1-ECA, HadGEM3-GC31-MM, NESM3, and TaiESM1) have larger trends than the observation (Figure S1d).

Prior to 2000, Arctic summer sea ice declined the fastest mainly in the sectors of the East Siberian, Chukchi, and Beaufort Seas as shown by the satellite observations (Figure 4a). After 2000, sea ice in these regions continued to decline, while the SIC in the sectors of the Laptev and Kara seas decreased much faster than the period before 2000, and even faster than in other sectors (Figure 4c). This explains the acceleration of the Arctic SIE decline in September after 2000. However, these observed changes in the spatial pattern of SIC trends are absent in CMIP6 MMM results (Figures 4b and 4d), so the faster SIE decline after 2000 is not reproduced in the CMIP6 simulations. Actually, the spatial patterns differ considerably among the CMIP6 models (Figure S3). The observed reduction of the SIC in the Laptev and Kara Seas sectors after 2000 is consistent with the trends of surface air temperature (Figure S4). Rapid atmospheric warming trends after 2000
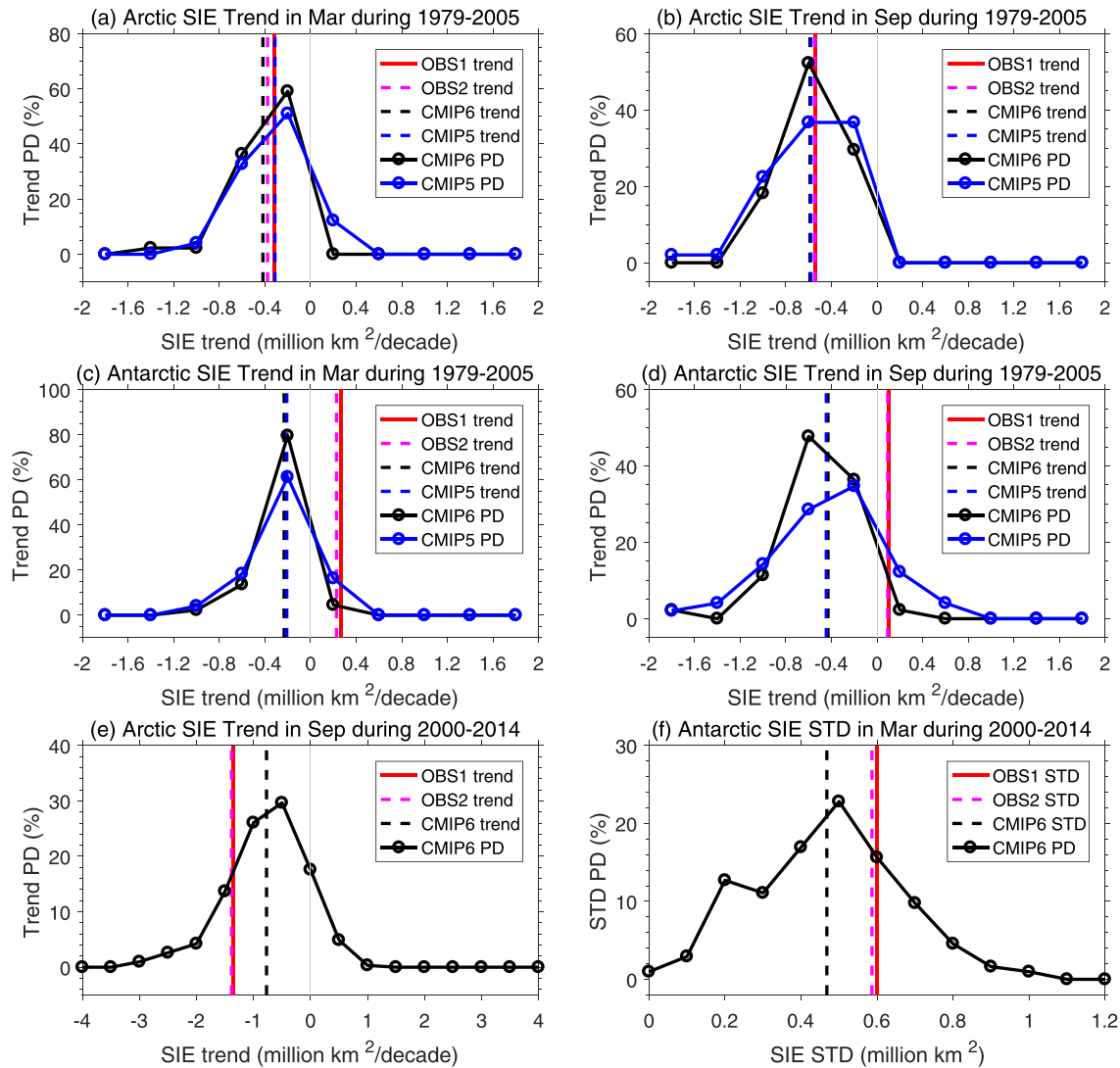
**Figure 3.** (a) Probability distribution (PD) of the linear trend of CMIP5/CMIP6-simulated March Arctic sea ice extent (SIE) for 1979–2005. (b) The same as (a) but for September. (c and d) The same as (a) and (b), but for the Antarctic. (e) PD of the linear trend of CMIP6-simulated September Arctic SIE for 2000–2014. (f) PD of March Antarctic SIE variability as represented by standard deviation (STD) for 2000–2014.

are present in the Laptev and Kara seas in the ERA5 reanalysis, but absent in the CMIP6 MMM result (Figure S4).

For the Antarctic, Figures 2c and 2d show that the temporal evolution of the MMM SIEs from CMIP6 and CMIP5 models is very similar for 1979 to 2005. One of the major problems faced by CMIP5 is that the observed weak but significant upward trend of Antarctic SIE cannot be reproduced (Turner et al., 2013; Shu et al., 2015). Our analysis reveals that this problem remains in CMIP6 models (Figures 2c, 2d, 3c, and 3d, Table 1, and Figure S2c): Both CMIP5 and CMIP6 models simulated negative Antarctic SIE trends instead of positive trends.

For annual mean Antarctic SIE during 1979–2005, the observed trends are 0.13 ($\pm$0.10) and 0.14 ($\pm$0.10) million $km^2$ per decade from UBremen and NSIDC, respectively (Table 1), and they exceed the 95% confidence level. However, trends from CMIP5 and CMIP6 are negative with values of $-0.34$ ($\pm$0.03) and $-0.35$ ($\pm$0.03) million $km^2$ per decade, respectively (Table 1). For March Antarctic SIE, the trends are 0.26 ($\pm$0.18) and 0.23 ($\pm$0.17) million $km^2$ per decade in UBremen and NSIDC observations, respectively, whereas both CMIP5 and CMIP6 have negative trends with values of $-0.21$ ($\pm$0.04) and $-0.23$ ($\pm$0.03) million $km^2$ per decade,
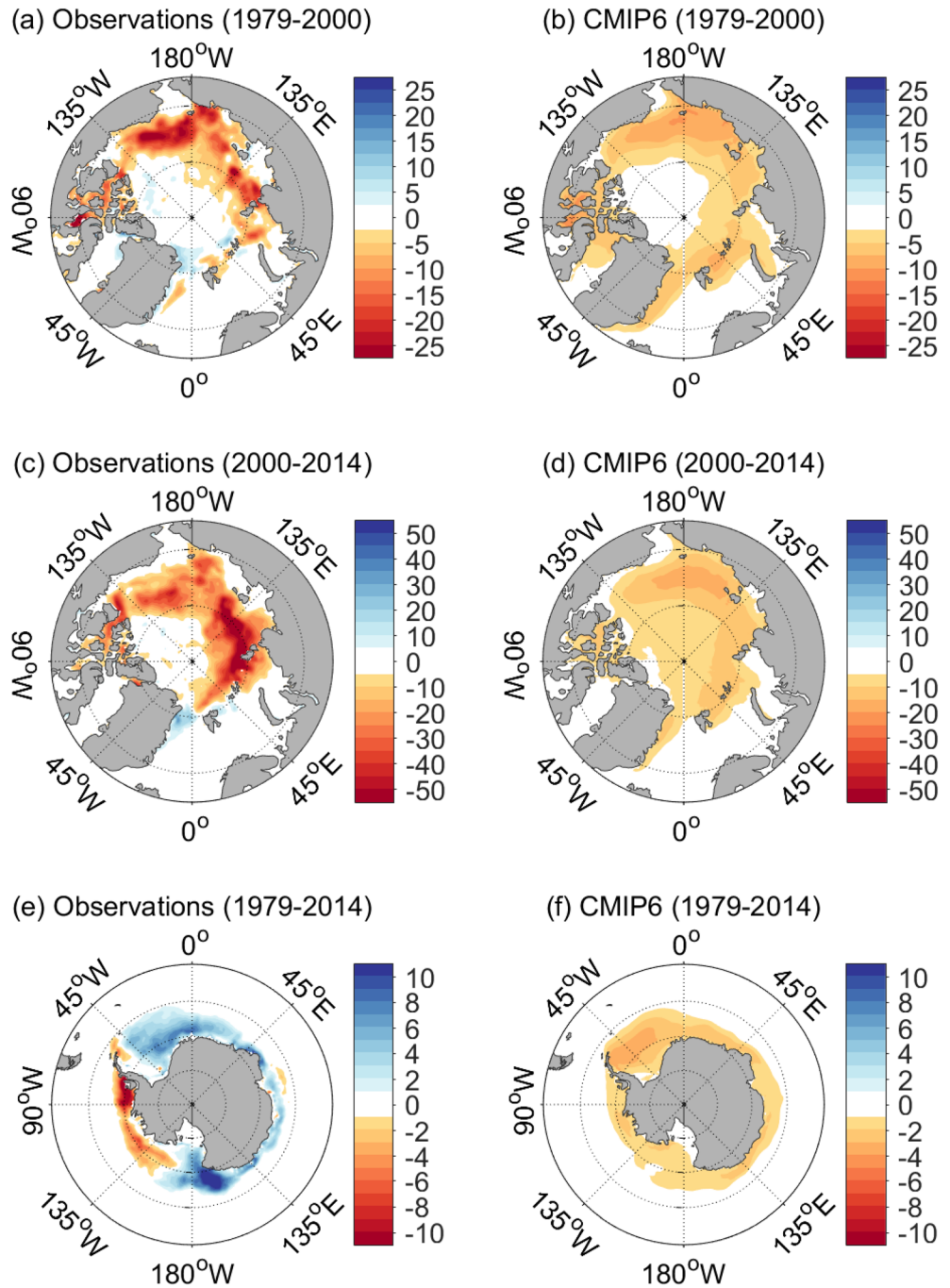
**Figure 4.** Linear trends of September Arctic and Autumn (MAM) Antarctic satellite-observed (left) and CMIP6-simulated (right) sea ice concentration (unit: % per decade). The observations are from NSIDC.

respectively. September trends from UBremen and NSIDC are both 0.10 ($\pm$0.16) million km$^2$ per decade and trends from CMIP5 and CMIP6 are $-0.45$ ($\pm$0.04) and $-0.43$ ($\pm$0.03) million km$^2$ per decade, respectively.

Previous studies show that the positive Antarctic SIE trend is largest in autumn (Shu et al., 2012, 2015) when SIC trends are negative in the Bellingshausen and Amundsen seas and positive in other regions (Figure 4e). However, the CMIP6 MMM has negative trends throughout the Antarctic (Figure 4f). Several models and some realizations have positive Antarctic SIE trends (Figures S2c, 3c, and 3d). We found that 11% (33 out

of 307) of CMIP6 realizations have positive SIE trends during 1979 to 2005 (Figure 3d). These 33 realizations are from 17 CMIP6 models (ACCESS-CM2, ACCESS-ESM1-5, BCC-CSM2-MR, BCC-ESM1, CAMS-CSM1-0, CNRM-ESM2-1, EC-Earth3-Veg, FGOALS-f3-L, GISS-E2-1-H, HadGEM3-GC31-MM, IPSL-CM6A-LR, MPI-ESM-1-2-HAM, MPI-ESM1-2-HR, MPI-ESM1-2-LR, MRI-ESM2-0, NESM3, and NorESM2-LM). Our further evaluation reveals that the spatial patterns of SIC trends in these 33 realizations are inconsistent with the observation (Figure S5), a finding the same as that for the CMIP5 (Shu et al., 2015).

Antarctic SIE has considerable interannual variability (Parkinson, 2019), which may influence the ability of climate models to reproduce observed Antarctic SIE trends (Polvani & Smith, 2013; Zunz et al., 2012). Figure 2c shows that the observed Antarctic March interannual variability between 2000 and 2014 is much larger than that prior to 2000 and is underestimated in CMIP6 models. The STDs of detrended March SIE for 2000–2014 (an indication of interannual variability) from Ubremen and NSIDC are 0.60 and 0.59 million $km^2$, while the mean value of the STDs from each CMIP6 realization is 0.47 million $km^2$ (Table 1). Figures 3f and S2d show that most of the CMIP6 realizations and models underestimate observed interannual SIE variability. Only six CMIP6 models (CanESM5, CanESM5-CanOE, CESM2-WACCM, CESM2-WACCM-FV2, GISS-E2-1-H, MRI-ESM2-0, and UKESM1-0-LL) have larger or similar interannual variability compared with the observations (Figure S2d). The reason why most CMIP6 models underestimate the interannual Antarctic SIE variability is unknown and needs to be investigated in future work.

Large intermodel spread in the sea ice trend was also a problem faced by CMIP5 models (Shu et al., 2015). Figures 3a–3d show that the intermodel spreads of both the Arctic and Antarctic SIE trends in CMIP6 models are reduced compared with those in CMIP5 models. For the Arctic, STDs of March SIE trends among the models are similar in CMIP5 and CMIP6 (0.25 and 0.24 million $km^2$ per decade, respectively). In September, however, they are very different between the CMIP5 and CMIP6 (0.34 and 0.26 million $km^2$ per decade, respectively). For the Antarctic, STDs of March SIE trends are 0.29 (CMIP5) and 0.19 million $km^2$ per decade (CMIP6), and those of September are 0.58 (CMIP5) and 0.33 million $km^2$ per decade (CMIP6). The smaller STDs in CMIP6 indicate an improvement stepping from CMIP5 models to CMIP6 models.

Considering the whole historical simulations of the CMIP6 for the satellite period (1979–2014), the MMM trend of Arctic SIE is $-0.70 \pm 0.06$ ($-0.82 \pm 0.18$ in the observation of the UBremen) million $km^2$ per decade for September and $-0.45 \pm 0.03$ ($-0.35 \pm 0.09$ in the observation) million $km^2$ per decade for March (Table 1). For the Antarctic, the MMM trend is $-0.43 \pm 0.02$ ($0.24 \pm 0.12$ in the observation) million $km^2$ per decade for September and $-0.23 \pm 0.02$ ($0.23 \pm 0.15$ in the observation) million $km^2$ per decade for March.

## 4. Conclusions

The SIEs simulated in CMIP6 models were evaluated in this study. We compared the CMIP6 simulations with the satellite observations and CMIP5 simulations.

For 1979–2005, performances of CMIP6 and CMIP5 models are very similar in the representations of SIE seasonal cycle and long-term trend for both hemispheres. Similar to CMIP5, CMIP6 MMM adequately reproduces the seasonal cycles of Arctic and Antarctic SIE, as well as the negative Arctic SIE trend. Models from both CMIP5 and CMIP6 obtain negative Antarctic SIE trends, which are inconsistent with the observed weak but significant positive trend. The biases of the mean SIE are slightly larger in the CMIP6 for both the hemispheres.

Although CMIP6 MMM results indicate a negative Antarctic SIE trend, positive trends are reproduced in 11% of CMIP6 (33 out of 307) realizations for 1979–2005. The percentage is 16% (8 out of 49 realizations) in the CMIP5 models analyzed by Shu et al. (2015). However, these CMIP5 and CMIP6 realizations are unable to reproduce the observed spatial pattern of SIC trends.

Large intermodel spreads also exist in CMIP6 models, but they are smaller than those in CMIP5 models. The reduction of the intermodel spread is found in the mean and seasonal cycle of the Antarctic SIE and the long-term SIE trends of both hemispheres. The intermodel spread of the Arctic SIE is slightly smaller in CMIP6 models than in CMIP5 models for summer, while it is similar between the two CMIP phases for the other seasons.

The CMIP6 models encounter some new challenges. During 2000–2014, Arctic summer sea ice declined faster than before, and Antarctic summer SIE had larger interannual variability. However, CMIP6 models did not reproduce these tendencies based on our assessment. In particular, Arctic September SIC in the sector of the Kara and Barents seas in the period of 2000–2014 has negative trends stronger than those in other Arctic regions, and stronger than those in the satellite period before 2000, which is not captured by the CMIP6 models. This causes the CMIP6 MMM trend of the Arctic September SIE to be slightly lower than the observed when considering the whole period of 1979–2014.

Part of the observed changes after 2000 might be due to internal climate variability, and we cannot expect all the short-term variations of sea ice to be simulated in the CMIP runs. Low-frequency climate variability can affect the sea ice trends for certain periods for both the Arctic and Antarctic (Castruccio et al., 2019; Mahajan et al., 2011; Polvani & Smith, 2013; Zhang et al., 2019; Zunz et al., 2012). On the one hand, it is important to document the recent changes in sea ice as reported in this study. On the other hand, we need more years to see whether the identified new tendencies are the consequence of the climate change or climate internal variability.

## References

Castruccio, F. S., Ruprich-Robert, Y., Yeager, S. G., Danabasoglu, G., Msadek, R., & Delworth, T. L. (2019). Modulation of Arctic Sea ice loss by atmospheric teleconnections from Atlantic multidecadal variability. *Journal of Climate*, *32*(5), 1419–1441. https://doi.org/10.1175/JCLI-D-18-0307.1

Cavalieri, D. J., Parkinson, C. L., Gloersen, P., & Zwally, H. J. (1996). *Sea ice concentrations from Nimbus-7 SMMR and DMSP SSM/I-SSMIS passive microwave data, version 1*. Boulder, Colorado USA: NASA National Snow and Ice Data Center Distributed Active Archive Center. https://doi.org/10.5067/8GQ8LZQVL0VL

Comiso, J. C., Gersten, R., Stock, L. V., Turner, J., Perez, G. J., & Cho, K. (2017). Positive trend in the Antarctic Sea ice cover and associated changes in surface temperature. *Journal of Climate*, *30*(6), 2251–2267. https://doi.org/10.1175/JCLI-D-16-0408.1

Comiso, J. C., Meier, W. N., & Gersten, R. (2017). Variability and trends in the Arctic Sea ice cover: Results from different techniques. *Journal of Geophysical Research: Oceans*, *122*, 6883–6900. https://doi.org/10.1002/2017JC012768

Copernicus Climate Change Service (C3S) (2017). ERA5: Fifth generation of ECMWF atmospheric reanalyses of the global climate. Copernicus Climate Change Service Climate Data Store (CDS), 20191120. https://cds.climate.copernicus.eu/cdsapp#!/home

Fetterer, F., Knowles, K., Meier, W. N., Savoie, M., & Windnagel, A. K. (2017). *Sea ice index, version 3*. Boulder, Colorado USA: NSIDC: National Snow and Ice Data Center. https://doi.org/10.7265/N5K072F8

Golaz, J. C., Caldwell, P. M., Van Roekel, L. P., Petersen, M. R., Tang, Q., Wolfe, J. D., et al. (2019). The DOE E3SM coupled model version 1: Overview and evaluation at standard resolution. *Journal of Advances in Modeling Earth Systems*, *11*(7), 2089–2129. https://doi.org/10.1029/2018MS001603

Holland, P. R. (2014). The seasonality of Antarctic sea ice trends. *Geophysical Research Letters*, *41*, 4230–4237. https://doi.org/10.1002/2014GL060172

Kwok, R., & Cunningham, G. F. (2015). Variability of Arctic sea ice thickness and volume from CryoSat-2. *Philosophical Transactions of the Royal Society A: Mathematical, Physical and Engineering Sciences*, *373*, 20140157. https://doi.org/10.1098/rsta.2014.0157

Mahajan, S., Zhang, R., & Delworth, T. L. (2011). Impact of the Atlantic Meridional Overturning Circulation (AMOC) on Arctic surface air temperature and sea ice variability. *Journal of Climate*, *24*(24), 6573–6581. https://doi.org/10.1175/2011JCLI4002.1

Maslanik J, Stroeve J, Fowler C., & Emery W. (2011). Distribution and trends in Arctic sea ice age through spring 2011. *Geophysical Research Letters*, *8*, L13502. https://doi.org/10.1029/2011GL047735

Olason, E., & Notz, D. (2014). Drivers of variability in Arctic sea-ice drift speed. *Journal of Geophysical Research: Oceans*, *119*, 5755–5775. https://doi.org/10.1002/2014JC009897

Parkinson, C. L. (2019). A 40-y record reveals gradual Antarctic sea ice increases followed by decreases at rates far exceeding the rates seen in the Arctic. *Proceedings of the National Academy of Sciences of the United States of America*, *116*(29), 14,414–14,423. https://doi.org/10.1073/pnas.1906556116

Parkinson, C. L., & Cavalieri, D. J. (2012). Antarctic sea ice variability and trends, 1979-2010. *The Cryosphere*, *6*(4), 871–880. https://doi.org/10.5194/tc-6-871-2012

Polvani, L. M., & Smith, K. L. (2013). Can natural variability explain observed Antarctic sea ice trends? New modeling evidence from CMIP5. *Geophysical Research Letters*, *40*, 3195–3199. https://doi.org/10.1002/grl.50578

Shu, Q., Qiao, F., Song, Z., & Wang, C. (2012). Sea ice trends in the Antarctic and their relationship to surface air temperature during 1979–2009. *Climate Dynamics*, *38*(11-12), 2355–2363. https://doi.org/10.1007/s00382-011-1143-9

Shu, Q., Song, Z., & Qiao, F. (2015). Assessment of sea ice simulations in the CMIP5 models. *The Cryosphere*, *9*(1), 399–409. https://doi.org/10.5194/tc-9-399-2015

Spreen, G., Kaleschke, L., & Heygster, G. (2008). Sea ice remote sensing using AMSR-E 89 GHz channels. *Journal of Geophysical Research*, *113*, C02S03. https://doi.org/10.1029/2005JC003384

Stroeve, J., Kattsov, V. M., Barrett, A. P., Serreze, M., Pavlova, T., Holland, M., & Meier, W. N. (2012). Trends in Arctic sea ice extent from CMIP5, CMIP3 and observations. *Geophysical Research Letters*, *39*, L16502. https://doi.org/10.1029/2012GL052676

Stroeve, J., & Notz, D. (2018). Changing state of Arctic sea ice across all seasons. *Environmental Research Letters*, *13*, 103001. https://doi.org/10.1088/1748-9326/aade56

Tatebe, H., Ogura, T., Nitta, T., Komuro, Y., Ogochi, K., Takemura, T., et al. (2019). Description and basic evaluation of simulated mean state, internal variability, and climate sensitivity in MIROC6. *Geoscientific Model Development*, *12*(7), 2727–2765. https://doi.org/10.5194/gmd-12-2727-2019

Turner, J., Bracegirdle, T. J., Phillips, T., Marshall, G. J., & Hosking, J. S. (2013). An initial assessment of Antarctic sea ice extent in the CMIP5 models. *Journal of Climate*, *26*(5), 1473–1484. https://doi.org/10.1175/JCLI-D-12-00068.1

Wei, T., Jian, L. I., Rong, X., Dong, W, Wu, B, & Ding, M. (2018). Arctic climate changes based on historical simulations (1900–2013) with the CAMS-CSM. *Journal of Meteorological Research*, *32*(6), 881–895. https://doi.org/10.1007/s13351-018-7188-5

Zhang, L., Delworth, T. L., Cooke, W., & Yang, X. (2019). Natural variability of Southern Ocean convection as a driver of observed climate trends. *Nature Climate Change*, *9*(1), 59–65. https://doi.org/10.1038/s41558-018-0350-3

Zunz, V., Goosse, H., & Massonnet, F. (2012). How does internal variability influence the ability of CMIP5 models to reproduce the recent trend in Southern Ocean sea ice extent. *The Cryosphere*, *7*(2), 451–468.